ELSEVIER

International Journal of Mass Spectrometry 194 (2000) 209–224

International Journal of Mass Spectrometry

Gas phase reactions of VO^+ with methyl methacrylates as studied by Fourier transform ion cyclotron resonance mass spectrometry

Adriana Dinca[a,*], Thomas P. Davis[b], Keith J. Fisher[a], Derek R. Smith[a], Gary D. Willett[a]

[a]*School of Chemistry and* [b]*School of Chemical Engineering and Industrial Chemistry, The University of New South Wales, Sydney NSW 2052, Australia*

Received 22 April 1999; accepted 24 June 1999

Abstract

Direct laser ablation of pressed vanadium pentoxide (V_2O_5) powder in the reaction cell of a Fourier transform ion cyclotron resonance (FTICR) mass spectrometer produces VO^+ as the only reproducible cation. This ion was reacted with methyl isobutyrate, methyl methacrylate, and methyl methacrylate dimer. Gas phase ion/molecule chemistry reveals that the complexity of the product distribution increases with the number of electron rich sites on the reagent molecule. Two sets of ion products are observed: (a) protonated reagent molecule and its corresponding stable fragment, formed by loss of CH_4O, and (b) products containing VO, formed by addition of whole reagent molecules and associated fragments. Products formed are a result of both consecutive and parallel reactions. Collision-induced dissociation (CID) experiments reveal that VO-whole molecule bonds are of a noncovalent nature. (Int J Mass Spectrom 194 (2000) 209–224) © 2000 Elsevier Science B.V.

Keywords: Fourier transform ion cyclotron resonance (FTICR) mass spectrometry; Laser ablation; Vanadium monoxide cation; Methyl isobutyrate; Methyl methacrylate; Ion–molecule reactions

1. Introduction

Gas phase reactions of vanadium oxide ions with neutral molecules are currently of interest [1–4], and are motivated by the importance of vanadium pentoxide as a catalyst in the oxidation of a variety of organic and inorganic molecules, where it is typically used as a substrate or support [5,6]. Catalytic processes at a surface may be mediated by local "ion-like" behavior of the substrate, so understanding the reactivity of the smaller ion entities, which can be obtained in gas phase, is of fundamental importance.

Methyl methacrylates have been in use since the 1930's [7], and they are typically produced via radical induced polymerization from the methyl methacrylate monomer [8]. Controlled polymerization processes to obtain monodisperse and/or low molecular mass polymers are currently of interest [9–12], thus studies involving well known catalysts such as vanadium pentoxide are well worth pursuing.

In this article we describe the use of Fourier transform ion cyclotron resonance mass spectrometry

* Corresponding author.

Dedicated to Professor Jim Morrison on the occasion of his 75th birthday.

PII S1387-3806(99)00136-0

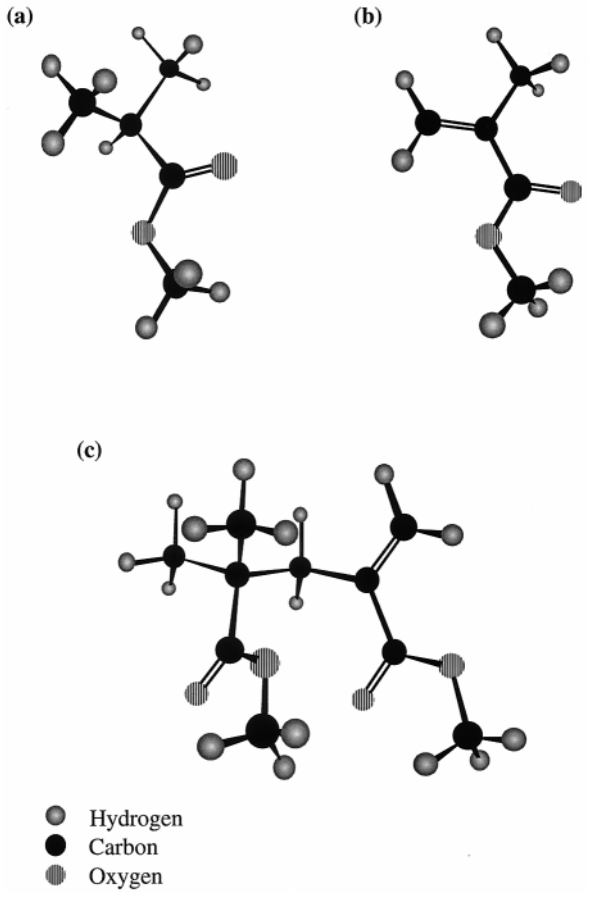

Fig. 1. Representations of structures of (a) methyl isobutyrate (mass = 102 u), (b) methyl methacrylate (mass = 100 u), (c) methyl methacrylate dimer (mass = 200 u).

(FTICR MS) to investigate the gas phase reactions of vanadium monoxide cation with the neutral reagents methyl isobutyrate (MIB), methyl methacrylate (MMA), and methyl methacrylate dimer (DMMA), representations of which are shown in Fig. 1. This is a complementary study to previous work [4] where vanadium oxide anion cluster reactions with methyl methacrylates were described. In the case of the anions no ion mediated polymerization process was observed. The reactivity of the anions decreases with increasing size, the reactions being driven by the large positive partial charge on an undercoordinated vanadium atom that interacts with a methoxy oxygen or a pair of conjugated double bonds on the reagent molecules. For anions with possible configurations that satisfy the preferred coordination of the vanadium atoms, no reactions were observed to take place for reaction times of up to 500 s.

FTICR MS has been widely and successfully used for two decades in the study of gas phase ion–molecule reactions [13,14]. Some of its more interesting applications are in the study of transition metal ions, transition metal hetero-atom ions, and their respective cluster ion reactivity towards organic molecules [13,15–28]. FTICR MS has the advantage of modeling low concentration situations, thus "expanding" the time scale to allow the observation and study of both intermediate and final products of a reaction. Studies of the reactivity of V_2O_5 as a substrate are typically conducted in the absence of solvents, a quality that this technique also affords.

Laser ablation has enabled us to produce the VO^+, VO_2^+, $V_2O_3^+$, and $V_2O_4^+$ ions. However, only VO^+ could reproducibly be obtained after multiple laser shots at the target. Thus we have studied the reactions of this cation with methyl methacrylate, methyl isobutyrate (which can be regarded as the saturated analogue of methyl methacrylate), and methyl methacrylate dimer.

2. Experimental

Vanadium pentoxide powder, the methyl isobutyrate, and the methyl methacrylate monomer were purchased from Aldrich. The vanadium pentoxide and the methyl isobutyrate were used as supplied, whereas the methyl methacrylate was purified by passing it through a column of basic alumina to remove the inhibitor, and then dried over calcium hydride.

The methyl methacrylate dimer (DMMA) was synthesized using a catalytic chain transfer polymerization [10] with azobis-isobutyronitrile (AIBN) as initiator and cobaltoxime boron trifluoride as the catalyst. The dimer was isolated in pure form by vacuum distillation using a Kugelrohr unit. The composition and purity of the three reagents was confirmed by electron/chemical ionization FTICR mass spectrometry.

The laser ablation FTICR mass spectra were obtained using a Spectrospin CMS-47 FTICR mass

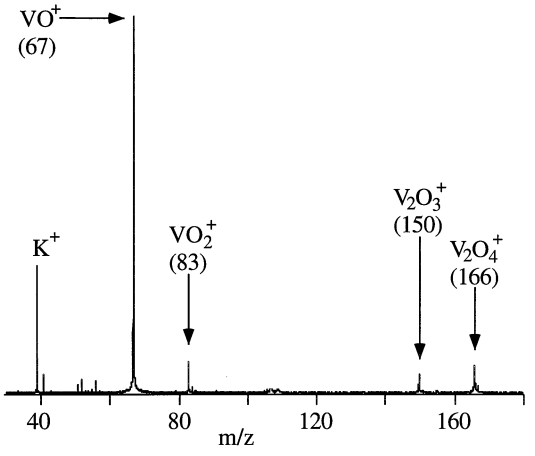

Fig. 2. Positive-ion laser ablation FTICR mass spectrum of vanadium pentoxide powder.

spectrometer equipped with a 4.7 T superconducting magnet [29,30]. The V_2O_5 powder was pressed into a hollowed out detachable, cylindrical stainless-steel satellite probe tip. The probe tip was inserted into a titanium single-section cylindrical ICR cell so that the V_2O_5 surface was close to the focus of the beam from a Spectra Physics DCR-11 Nd:YAG laser [30]. The background pressure was allowed to stabilize around 2×10^{-9} mbar prior to admission of the reagent vapor (MIB, MMA, or DMMA) and of argon cooling gas. The reagent was leaked into the ultrahigh vacuum chamber housing the ICR cell, using its normal vapor pressure at room temperature, through a Balzers molecular leak valve, and allowed to stabilize at an uncorrected background pressure of 1×10^{-7} mbar. Argon gas was also leaked into the ultrahigh vacuum chamber through a second Balzers molecular leak valve, and the gases were allowed to stabilize at a combined and uncorrected total pressure of 3×10^{-7} mbar, as measured by a Bayard-Alpert gauge.

The laser ablation experiments were performed with the focused beam (through a lens of focal length of 110 mm and spot diameter on the sample of 0.2 mm) of a Nd:YAG laser (1064 nm, 8 ns) at power densities in the range of 0.1–2000 $MWcm^{-2}$.

The event sequence for the laser ablation FTICR mass spectrometry experiments has been described in detail elsewhere [4]. In short, the ICR cell is cleared of any ions remaining from a previous experiment by inversion of the voltage on one of the trapping plates followed by a short delay of 5 s. The leading edge of a pulse of 10 ms is used to trigger the 8 ns Nd:YAG laser pulse in the Q-switch mode, after which a second delay (of between 1 and 2 s) allows for most of the ablated neutral species to be pumped away, as well as for radiative and collisional cooling of the ions trapped in the ICR cell by a combination of magnetic and electric fields. Ion selection is performed by using broadband sweep ejection and single rf shots at selected frequencies, followed by another delay (of between 1 and 4 s) to allow further cooling of the ions selected. A second selection of the ions of interest is then performed, after which the ions are allowed to react with the reagent gas for a fixed period of time. This experiment was repeated for reaction times of between 0 and 500 s. After the elapsed reaction time, a 10 μs rf chirp pulse (135 V applied to each excitation plate 180 ° out of phase) was used to bring all the ions in the ICR cell into phase-coherent motion, followed by detection of all the ions in the cell and spectrum acquisition. Ions were trapped in the cell by potentials applied to the trapping plates in the range of 3.5–4.0 V.

Identification of the products of reaction was aided by collision-induced dissociation (CID) experiments [31,32]. Generation, cooling, and selection of the parent ion (VO^+) was performed, followed by formation of the product ions. Of these, the ion of interest was then isolated and accelerated by an rf pulse at the appropriate frequency, of duration between 10 and 50 μs. After allowing an average of 1–2 collisions of the ions with the argon atoms to occur, a spectrum was recorded. MS^n experiments were conducted as well, in an attempt to elucidate pathways of reactions.

Ab initio density functional theory calculations using GAUSSIAN 98W [33] at the B3LYP [34–37] level of theory were used to optimize the structure of VO^+ ion, and to determine partial charges on the two atoms for the lowest energy triplet, singlet, and quintuplet states. These calculations used a 6-311G basis set with (d,p) polarization functions. Preliminary ab initio molecular orbital calculations (using GAUSSIAN 98W) at the Hartree–Fock level of theory using the 3-21G

basis set were used to gain insight into stable structures of some of the protonated reagent molecules formed during the monitored reactions ([MMA + H]$^+$ and [DMMA + H]$^+$).

3. Results and discussion

Laser ablation of the V_2O_5 sample in the positive-ion mode produced VO^+, VO_2^+, $V_2O_3^+$, and $V_2O_4^+$ ions, and a typical FTICR mass spectrum obtained by laser ablation of a fresh vanadium pentoxide surface is shown in Fig. 2. Only the VO^+ could be reliably produced and isolated after multiple shots at the same spot on the target. Reactions of VO^+ with each of the three reagents (MIB, MMA, and DMMA) were observed and analyzed.

The vanadium monoxide cation reacts with all the reagents studied (MIB, MMA, and DMMA) and typical spectra for intermediate and final product distributions are shown in Figs. 3, 4, and 5, respectively. Two classes of final products are observed to form in each of these reactions:

(a) protonated reagent (R) molecules:
   (i) [R + H]$^+$ in the case of DMMA;
   (ii) proton bound dimers [R + H + R]$^+$ in the case of MIB and MMA;
   (iii) as well as the corresponding stable fragment [(R + H)−CH_4O]$^+$ obtained by loss of methanol from the protonated reagent molecule [R + H]$^+$ in the case of each of the reagents.

(b) VO containing ions, formed by consecutive addition of reagent molecules, as well as by fragmentation of primary products (first step), and ligand exchange reactions. The product distribution and complexity of reaction increases with the number of electron rich sites on the reagent molecule.

3.1. Methyl isobutyrate

The reaction with methyl isobutyrate is the simplest VO^+ has with the three reagents (see Fig. 3). The final major products correspond to the two classes described above. For group (a), the formation of the protonated complex [MIB + H]$^+$ and protonated fragment [(MIB + H)−CH_4O]$^+$ occur simultaneously, with the latter being produced in larger quantity. The protonated complex then goes on to add another MIB molecule, to form the final stable product, the proton bound dimer [MIB + H + MIB]$^+$. There is evidence of slow disappearance of the protonated fragment concomitant with an increase in the production of the protonated dimer [MIB + H + MIB]$^+$. This is indicative of a chemical ionization reaction with a relatively slow rate, which produces more protonated MIB molecules, which then further the production of the proton bound dimer.

For the group (b) class of reactions between VO^+ and MIB there are two final products containing VO:

(i) one is formed by the consecutive addition of three MIB molecules to VO^+ to form the final product [$VO(MIB)_3$]$^+$, and

(ii) the other by the formation of [VO(MIB−CH_3)]$^+$ followed by the consecutive addition of two more MIB molecules to form the intermediate and final products [VO(MIB)(MIB−CH_3)]$^+$ and [$VO(MIB)_2$(MIB−CH_3)]$^+$, respectively.

Reaction profiles describing the development of these reactions are shown in Fig. 6, and are grouped into three categories, representing the main reaction channels, in order to illustrate the different parallel processes taking place as well as their steps: production and evolution of protonated MIB and its protonated fragment [Fig. 6(a)], as well as the appearance of the proton bound dimer; production of VO^+ containing products, by consecutive addition of MIB molecules, with loss in the first step of the reactions described in (b)(ii) of a methyl group [Fig. 6(b) and (c)].

3.2. Methyl methacrylate

In the reaction with methyl methacrylate, VO^+ behaves more aggressively than in the previously described reaction with MIB, producing four major final products containing VO. These are based on the formation of the [VO(MMA)]$^+$ and [VO(R)]$^+$ complexes, where R is [CH_2O], [MMA−CH_2O], and

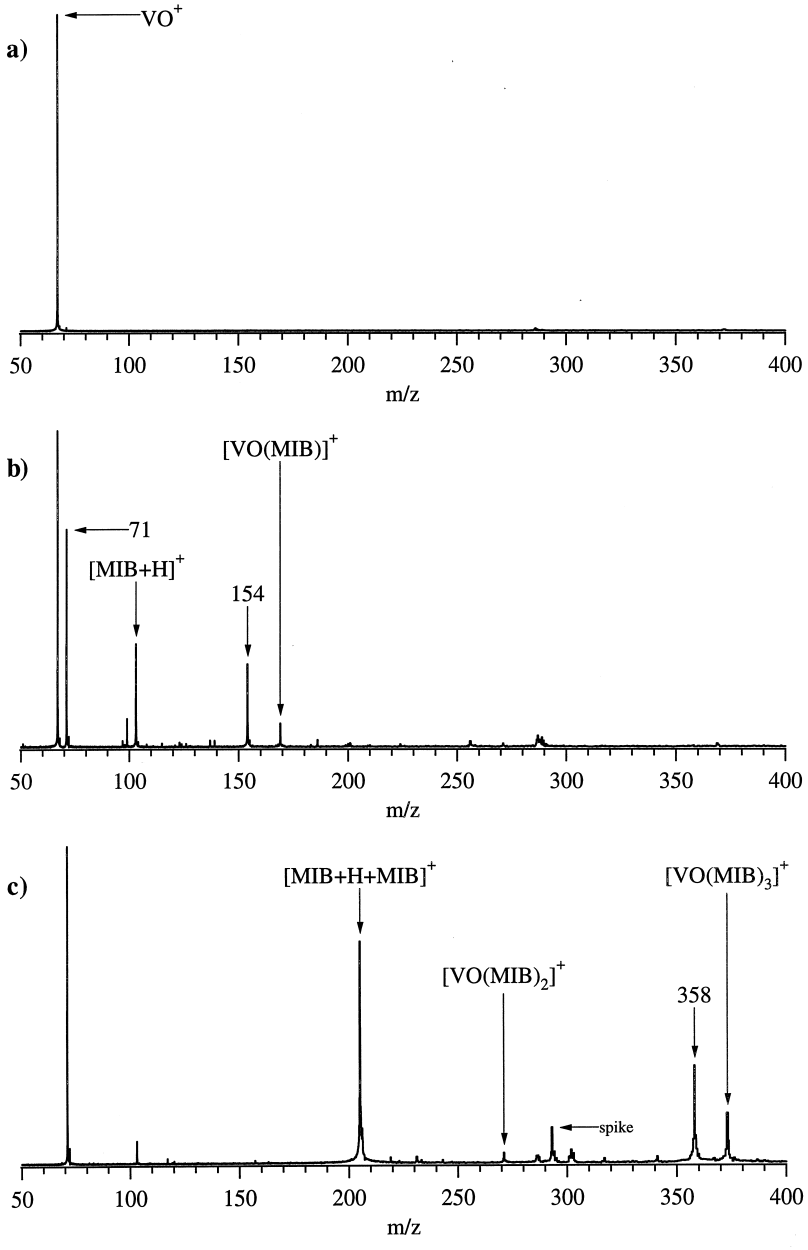

Fig. 3. FTICR mass spectra of the products of VO^+ reaction with methyl isobutyrate after a reaction time of (a) 0 s, (b) 1 s, (c) 100 s. Possible assignment for $m/z = 71$ is $[(MIB + H)-CH_4O]^+$; for $m/z = 154$ is $[VO(MIB\text{-}CH_3)]^+$; for $m/z = 358$ is $[VO(MIB)_2(MIB-CH_3)]^+$.

$[MMA-CH_3]$. These initial products then each undergo addition of two more MMA molecules, as shown in Figs. 4 and 7, where these four reaction channels are presented: formation of $[VO(CH_2O)]$ adduct cation, followed by successive addition of two more MMA molecules [Fig. 7(a)]; formation of $[VO(MMA-CH_2O)]$ adduct cation [thus addition of the complement fragment from MMA as compared to the reaction described in 7(a)], followed by addition of two more MMA molecules [Fig. 7(b)]; formation

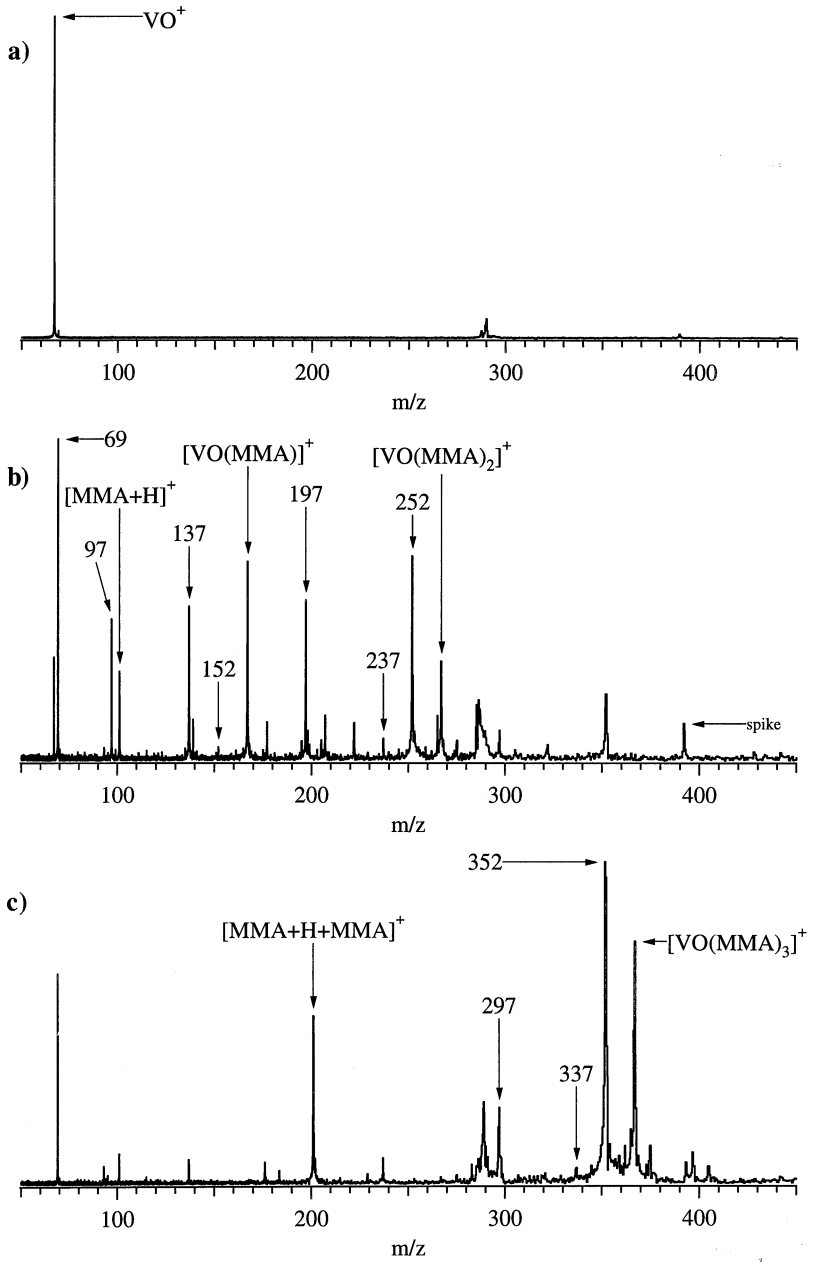

Fig. 4. FTICR mass spectra of the products of VO^+ reaction with methyl methacrylate after a reaction time of (a) 0 s, (b) 2 s, (c) 100 s. Possible assignment for m/z = 69 is $[(MMA + H)-CH_4O]^+$; for m/z = 97, 197, and 297 are $[VO(CH_2O)]^+$, $[VO(MMA)(CH_2O)]^+$, and $[VO(MMA)_2(CH_2O)]^+$, respectively; for m/z = 137, 237, and 337 are $[VO(MMA-CH_2O)]^+$, $[VO(MMA)(MMA-CH_2O)]^+$, and $[VO(MMA)_2(MMA-CH_2O)]^+$, respectively; for m/z = 152, 252, 352 are $[VO(MMA-CH_3)]^+$, $[VO(MMA)(MMA-CH_3)]^+$, and $[VO(MMA)_2(MMA-CH_3)]^+$, respectively.

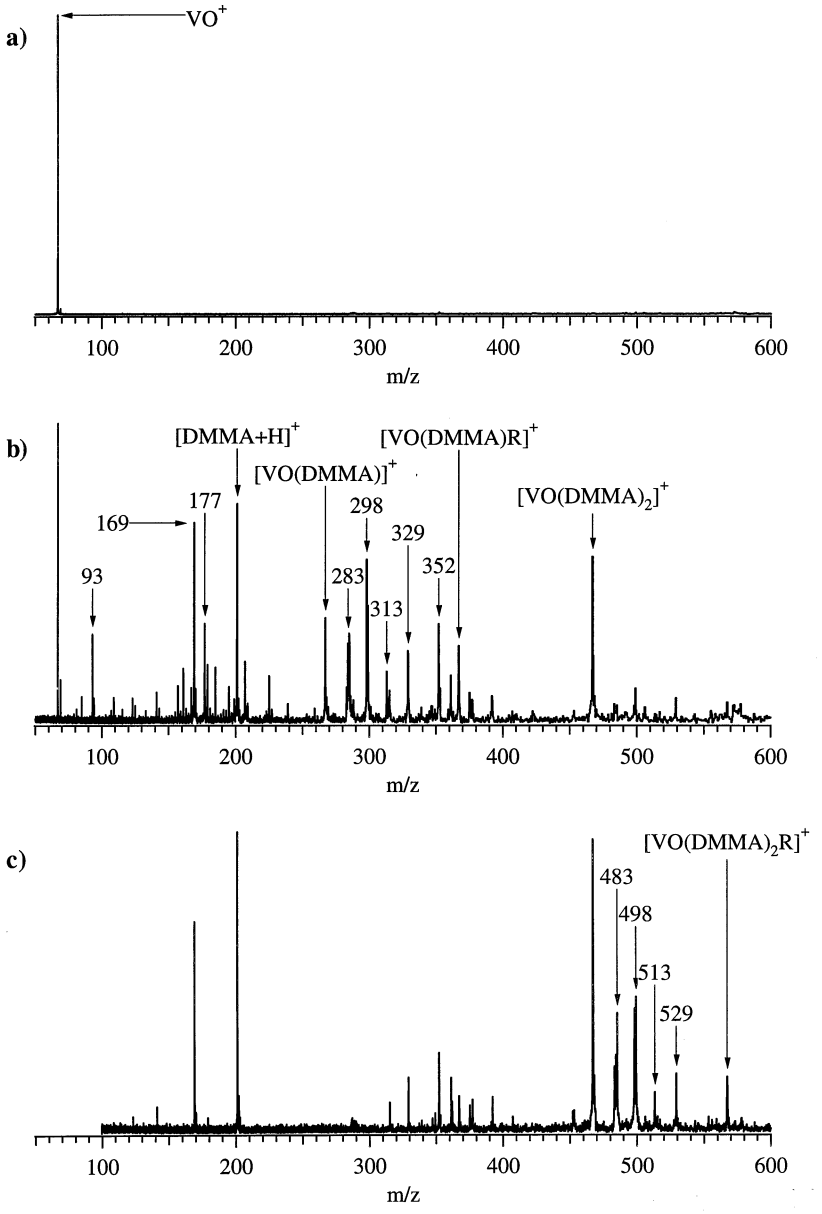

Fig. 5. FTICR mass spectra of the products of VO^+ reaction with methyl methacrylate dimer after a reaction time of (a) 0 s, (b) 5 s, (c) 100 s. Possible assignment for *m/z* = 169 is $[(DMMA + H)-CH_4O]^+$; for *m/z* = 283 and 483 are $[VO(DMMA)O]^+$ and $[VO(DMMA)_2O]^+$; for *m/z* = 298 and 498 are $[VO(DMMA)(CH_3O)]^+$ and $[VO(DMMA)_2(CH_3O)]^+$; for *m/z* = 313 and 513 are $[VO(DMMA)(C_2H_6O)]^+$ and $[VO(DMMA)_2(C_2H_6O)]^+$ for *m/z* = 329 and 529 are $[VO(DMMA)(CH_3O)_2]^+$ and $[VO(DMMA)_2(CH_3O)_2]^+$; for *m/z* = 352 is $[VO(DMMA)R-CH_3]^+$, where R(*m/z* = 100) is, most likely, [MMA].

of $[VO(MMA-CH_3)]$ adduct cation, followed by the addition of two more MMA molecules [Fig. 7(c)]; and simple consecutive addition of three MMA molecules to the VO cation [Fig. 7(d)].

The proton bound dimer $[MMA + H + MMA]^+$ and fragment of the protonated monomer, $[(MMA + H)-CH_4O]^+$ are also produced, the mechanisms paralleling those for the equivalent reactions in the case

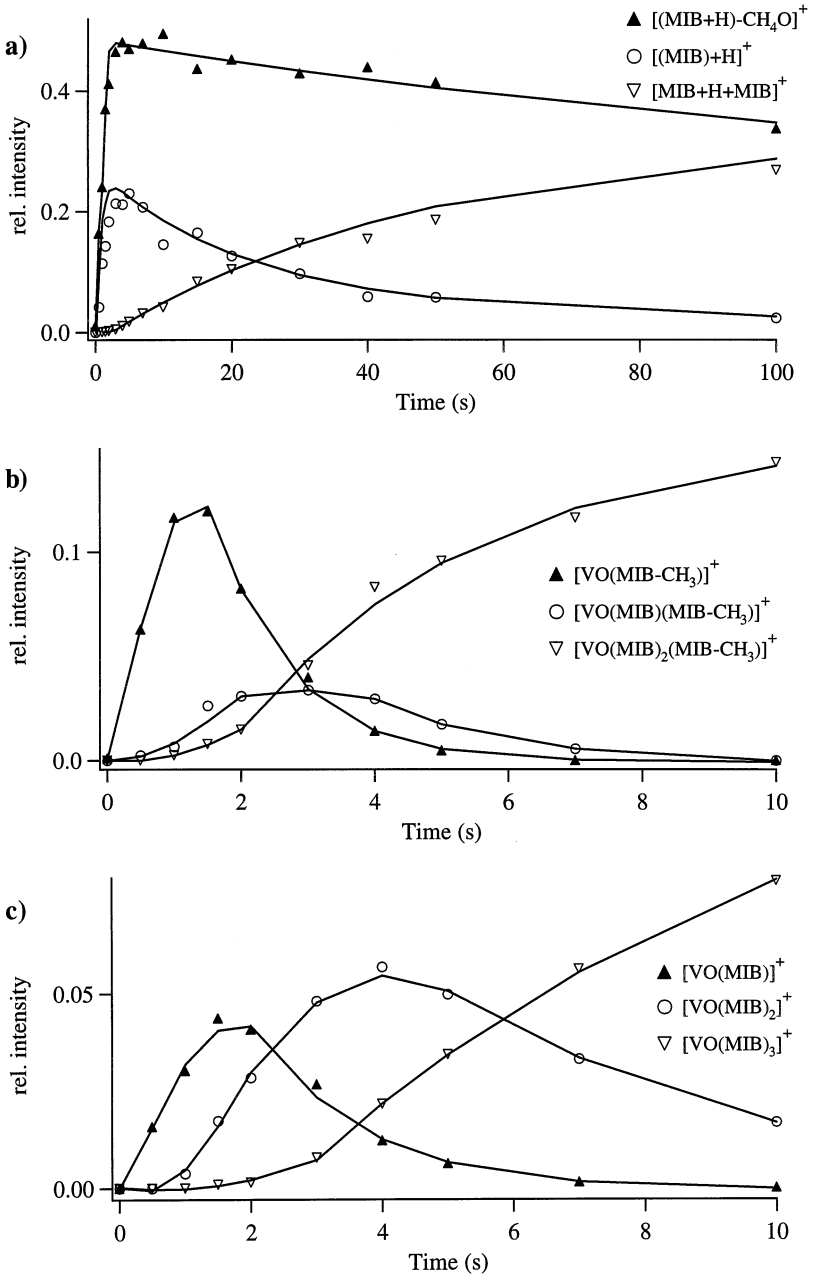

Fig. 6. Reaction profiles of VO^+ reaction with methyl isobutyrate. Relative intensities are with respect to the total abundance of ions present in the spectrum at the given time, total relative abundance being 1.

of MIB. CID experiments reveal that the ion of *m/z* 201 [as seen in Fig. 4(c)] is indeed a proton bound dimer, and not the protonated methyl methacrylate dimer molecule. The dissociation patterns of these two ions are different: $[MMA + H + MMA]^+$ loses a MMA molecule to form $[MMA + H]^+$, whereas $[DMMA + H]^+$ loses groups such as CH_4O and $HCOOCH_3$. Thus no polymerization processes occur

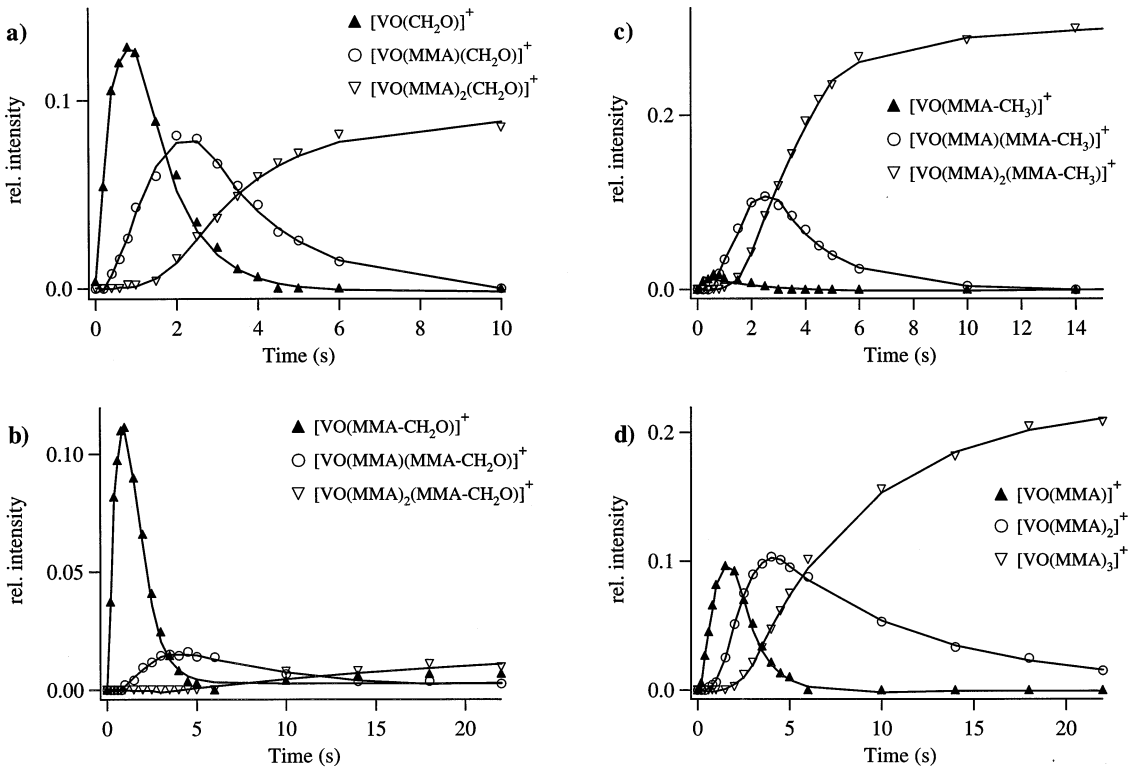

Fig. 7. Reaction profiles of VO^+ reaction with methyl methacrylate. Relative intensities are with respect to the total abundance of ions present in the spectrum at the given time, total relative abundance being 1.

paralleling the radical induced polymerization of MMA to produce DMMA. A schematic diagram describing the most likely reaction pathways of VO^+ with MMA is shown in Fig. 8.

3.3. Methyl methacrylate dimer

The reaction of VO^+ with the methyl methacrylate dimer produces the largest number of products (as can be seen in Fig. 5). The reaction profiles describing the production of $[DMMA + H]^+$ and $[(DMMA + H)-CH_4O]^+$ are shown in Fig. 9(a). These profiles do not indicate the presence of a chemical ionization process to form $[DMMA + H]^+$ from $\{[(DMMA + H)-CH_4O]^+ + DMMA\}$ or of $[(DMMA + H)-CH_4O]^+$ from $[DMMA + H]^+$. After ~5 s reaction time, no change in the relative abundance of these two products is observed (for reaction times of up to 500 s), indicating that the proton affinity of DMMA is larger than that of $[DMMA-CH_4O]$. No proton bound dimers of DMMA are observed.

Ab initio calculations at the Hartree–Fock level of theory using the 3-21G basis set reveal several structures corresponding to local minima for the protonated MMA and DMMA molecules. In the case of $[MMA + H]^+$, the optimized structure lowest in energy indicates interaction of the proton with one of the lone electron pairs of the carbonyl oxygen [distance $r(O-H^+) = 0.97$ Å], the proton being coplanar with the carbon–oxygen frame of the molecule [{$D(O–C=O–H^+) = 180.0°$}, $A(C=O–H^+) = 120.2°$]. In the case of $[DMMA + H]^+$, the proton interacts with a lone electron pair of the carbonyl oxygen of the conjugated double bonds (R(O–H) = 1.08 Å), with the other carbonyl oxygen in close proximity (R(O–H) = 1.336 Å), with the three atoms being almost collinear

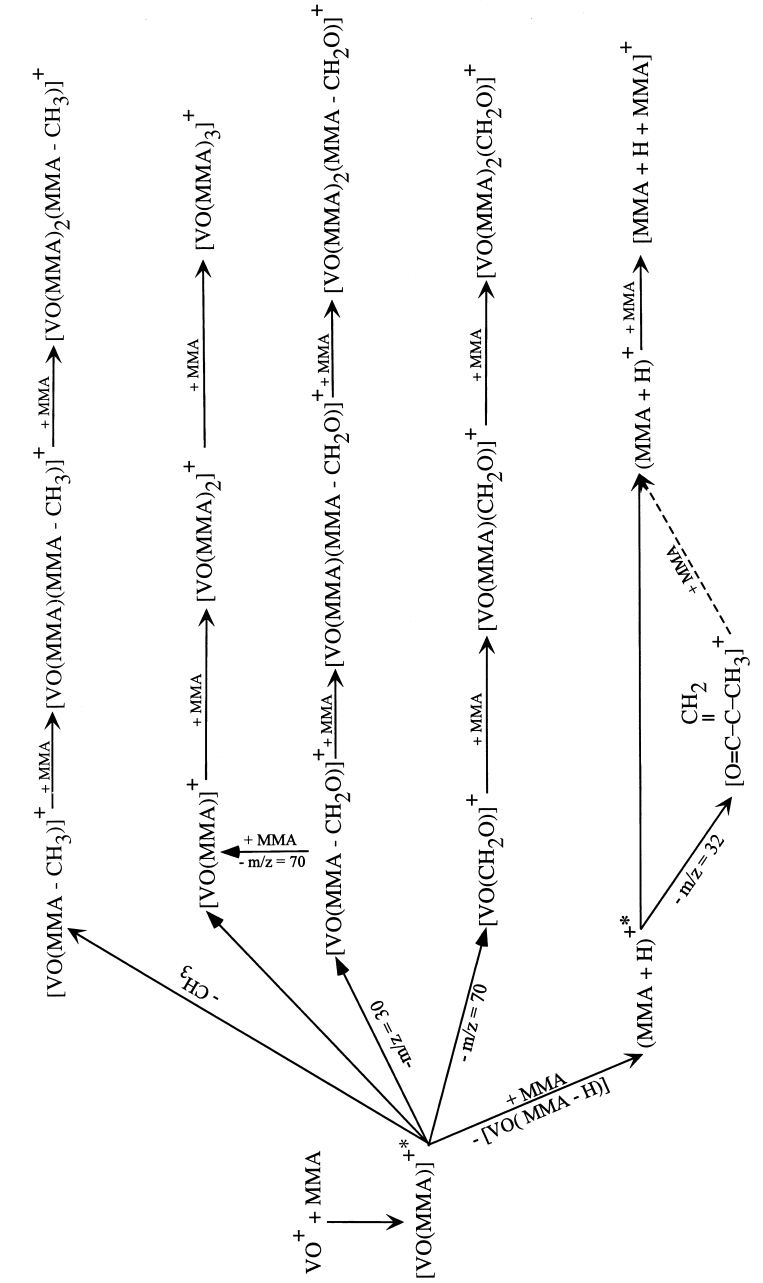

Fig. 8. Schematic representing reaction pathways in the reaction of VO^+ with MMA. Dashed arrows represent minor or possible pathways, whereas solid arrows represent observed major pathways. Possible formulae for fragments are: for $m/z = 70$, $CH_3C(CH_2)COH$; for $m/z = 30$, CH_2O; for $m/z = 32$, CH_4O.

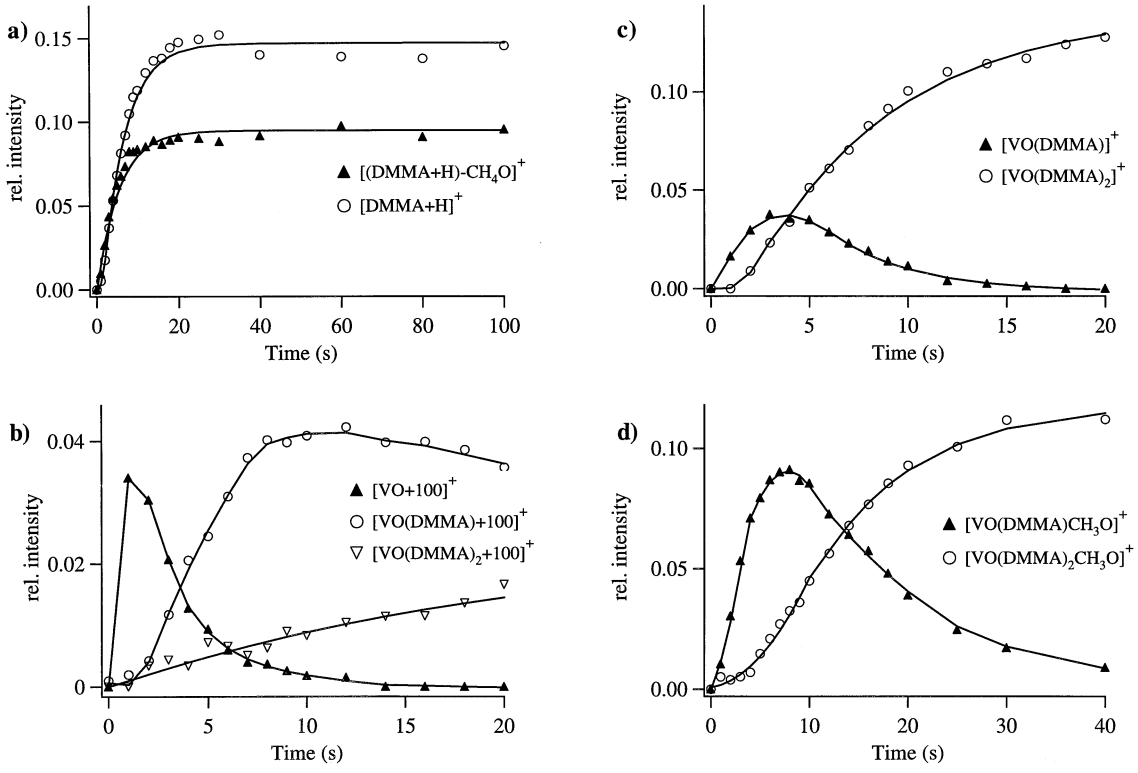

Fig. 9. Reaction profiles of VO^+ reaction with methyl methacrylate dimer. Relative intensities are with respect to the total abundance of ions present in the spectrum at the given time, total relative abundance being 1.

(A(O-H^+-O) = 168.0°). Based on these calculations, we conclude that in the formation of $[R + H + R]^+$ where R is MIB or MMA, the proton is most likely bound to the carbonyl oxygens on each of the two reagent molecules. In the case of $[DMMA + H]^+$ the calculations indicate that the proton is bound to the carbonyl oxygen of the conjugated double bonds, with the other carbonyl oxygen in close proximity. This together with steric hindrance explains the lack of proton bound dimers of DMMA being observed.

Reaction profiles describing the formation of some of the VO containing products from the reaction of VO^+ with DMMA are shown in Fig. 9: formation of $[VO + 100]^+$, (most likely $[VO(MMA)]^+$) via a depolymerization step, followed by the addition to this complex of two more DMMA molecules [Fig. 9(b)]; simple consecutive addition of two DMMA molecules [Fig. 9(c)]; and formation of what is most likely $[VO(DMMA)(CH_3O)]^+$, probably from the decomposition of a larger ion, followed by the addition of another DMMA molecule [Fig. 9(d)]. Thus all of the final products include a DMMA molecule—most of them two. Some of the products also contain fragments of a DMMA molecule, such as $[CH_3O)]$, $[(CH_3O)_2]$, [O], $[C_2H_6O]$, $[DMMA-CH_3]$, and a fragment of $m/z = 100$ (probably MMA). A diagram of the most likely reaction pathways is shown in Fig. 10.

Some of the observed final product ions from the reactions studied were isolated in the presence of the reagent and argon gases, and allowed to undergo further reactions and/or fragmentation. The spectra obtained in these experiments indicate that these species are all stable to further reaction with MIB, MMA, and DMMA, respectively, as well as to dissociation. Exchange reactions between whole reagent

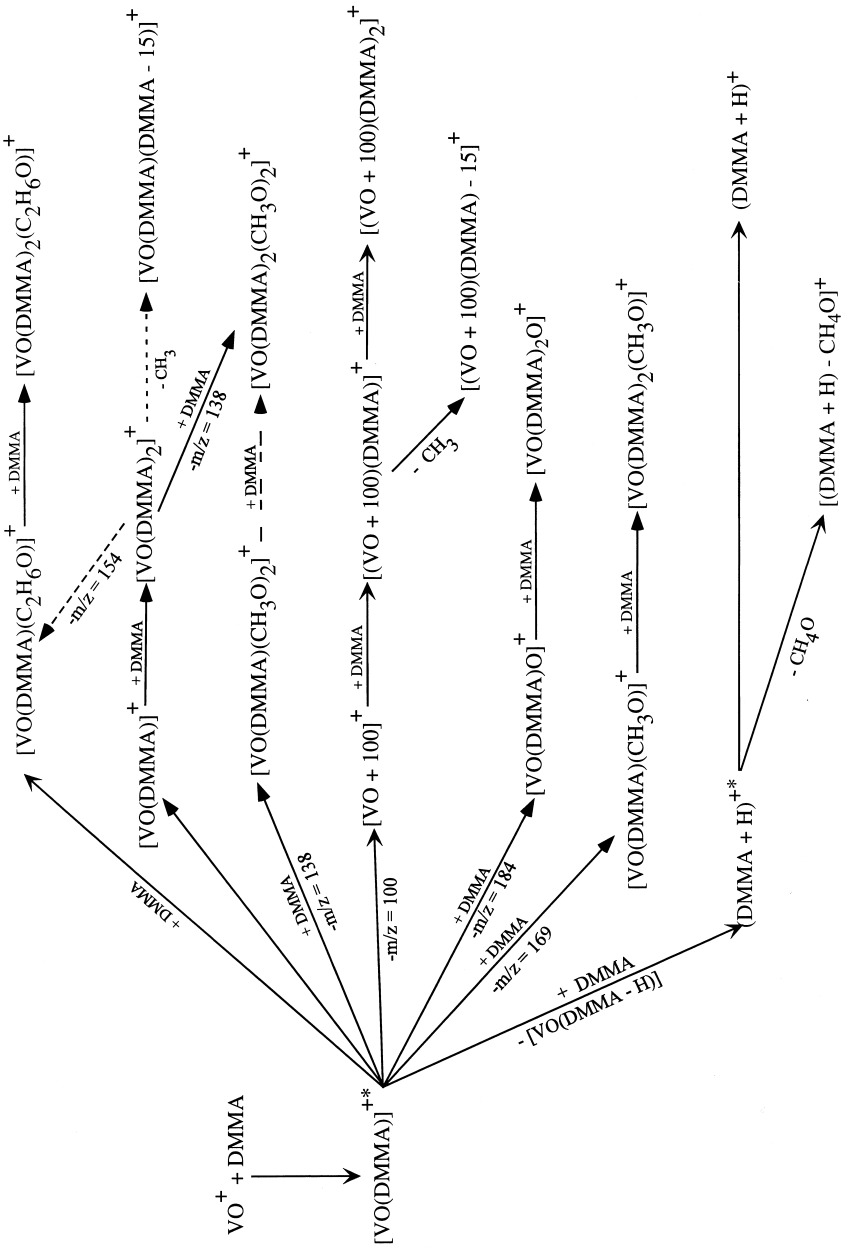

Fig. 10. Schematic representing reaction pathways in the reaction of VO^+ with DMMA. Dashed arrows represent minor or possible pathways, whereas solid arrows represent observed major pathways. Possible formulae for fragments are: for $m/z = 169$, [DMMA−CH_3O]; for $m/z = 154$, [DMMA−(CH_3O)−(CH_3)]; for $m/z = 138$, [DMMA−2(CH_3O)]; for $m/z = 184$, [DMMA−O]; for $m/z = 100$ [MMA].

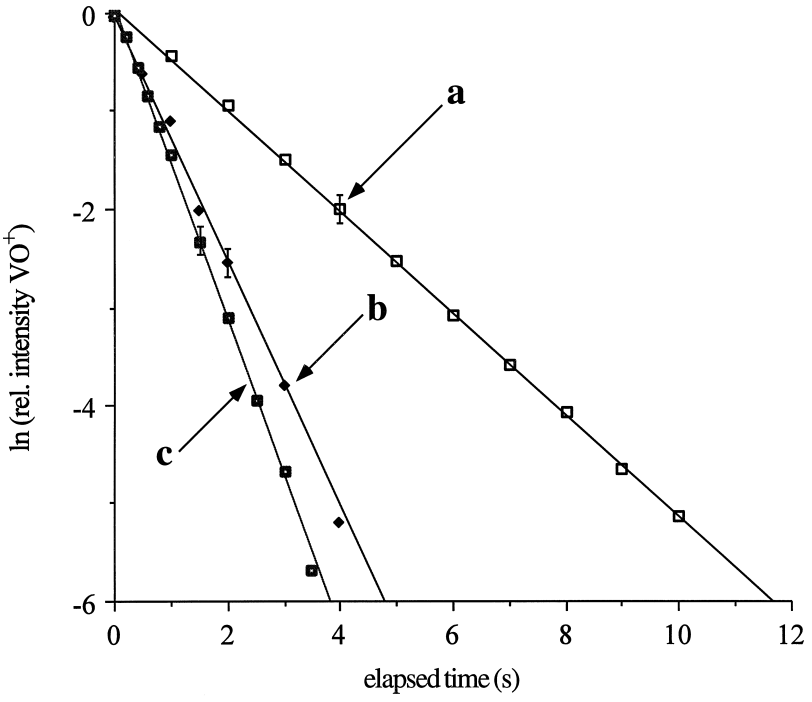

Fig. 11. VO^+ decay profiles in reactions with (a) DMMA, (b) MMA, and (c) MIB, respectively. The decay of the VO^+ ion in each case describes a pseudo-first order reaction. Correction factors for the reagent gases were not available, thus absolute rates were not extracted.

molecules bound to the final product and reagent molecules in the background could occur; however, our experiments cannot differentiate between such processes and no reaction. CID measurements were carried out when feasible (if the product ion analyzed was present in significant quantity) for some of the product ions. However, because of the large distribution of products in some cases, it was not always successful. In general, the CID FTICR mass spectra obtained indicate loss of entire reagent molecule(s).

4. General discussion

The reactions with the three reagents are similar in the type of products observed. As previously mentioned, two major classes of products are formed via both consecutive and parallel processes, as described in the schematics presented in Figs. 8 and 10. However, in each of the three reactions, the decay of the parent ion relative abundance, VO^+, follows a pseudo-first order rate (for not less than 99% of the reaction), as seen in Fig. 11. This is indicative of a single process being responsible, in each case, for the depletion of the parent vanadium monoxide cation.

The appearance of all the first step products, i.e. the protonated reagent molecules $[R + H]^+$, their associated fragments $[(R + H)-CH_4O]^+$, and VO containing molecules $[VO + L]^+$ where R is MIB, MMA, or DMMA and L is either R or a fragment of it, is on a similar time scale. This, together with the decay profile of the vanadium monoxide parent ion, allows us to postulate that the parent ion depletion process is due to formation of an addition intermediate complex $[VO + R]^+*$, where R is MIB, MMA, or DMMA, respectively, which then follows one of two major pathways:

(a) Upon collision with (most likely) a neutral reagent molecule, a protonated complex $[R + H]^+*$ is formed, possibly via proton transfer from the intermediate complex ion ($[VO + R]^+*$) to the neu-

tral reagent molecule (R) with which it collides. Some of these new ions (i.e. $[R + H]^{+}$*) decay by loss of CH_4O, whereas in the case of MIB and MMA, the remainder undergo the addition of another reagent molecule to form the stable final proton bound dimer product.

(b) The $[VO + R]^{+}$ complex either: (1) relaxes by photoemission or by collision with background molecules, or (2) relaxes by loss of a fragment of the added reagent molecule. In each of the reactions studied, the VO containing "relaxed" ion undergoes further reactions, typically two more, by addition of another two reagent molecules. In the case of DMMA some decay of intermediate products is also observed.

The appearance of the $[R + H]^{+}$ and $[(R + H)-CH_4O]^{+}$ where R is MIB, MMA, or DMMA is a relatively fast process [see e.g. in Figs. 6(a) and 9(a)], and is the result of at least two consecutive reactions, because neither can be obtained from a one step reaction between VO^{+} and R. The production time for the formation of these products is comparable to the delay times used in our experiments—delay times (typically of between 2 and 4 s total) that allow the cooling of the parent ion prior to its selection, isolation, and start of the monitored reaction. Thus we expect that most of the VO^{+} ions produced upon laser ablation and with electronic excited states of higher energy than the energy of the ionized reagent molecules (please see Sec. 6 for details on the ionization energy of the reagents, as well as excited states of VO^{+}) would have already reacted via a charge transfer reaction. Therefore, the electronic energy distribution in the remaining VO^{+} ions should not contain any excited states that would favor a charge transfer reaction. This, together with the fact that no R^{+} ions where R is MIB, MMA, or DMMA were observed to form during the monitored reactions, is the basis of the proposed model for the reaction pathways.

The sizes of the final products are probably determined by the preferred coordination of the vanadium atom as well as by steric crowding. The interaction with the reagent molecules is proposed to occur via the vanadium atom because this has a large positive charge concentrated on it [partial Mulliken charge on the vanadium atom estimated at around +1.3 by B3LYP/6-311G(d,p) calculations], to either the methoxy oxygen, or the electron rich carbonyl-alkene conjugated double bonds, in the case of MMA and DMMA. This conclusion is supported by the composition of the observed products. Preference of interaction with a lone electron pair on the methoxy oxygen versus the double bonds probably is determined by the electronic state of VO^{+} (please see Sec. 6 for details of electronic states of VO^{+}). Thus we propose that in products of the type [VO + reagent molecule fragment(s)] and [VO + reagent molecule fragment(s) + whole reagent molecule(s)], binding of the reagent molecule fragment(s) to VO is via the methoxy oxygen, whereas the interaction with whole reagent molecules for products of the type [VO + whole reagent molecule(s)] and [VO + reagent molecule fragment(s) + whole reagent molecule(s)] could also be the result of interactions with the π-electron system of the conjugated double bond(s).

CID experiments on the VO containing final and intermediate products show, for the most part, the loss of entire reagent molecules (with little kinetic energy given), or entire added reagent molecule fragment to eventually give the VO^{+} ion—not a surprising fact, considering the strength of the V^{+}–O bond (5.99 eV [38]). This suggests that the bonds in the addition complex $[VO(R)]^{+}$, between VO and the reagent molecule (R) are not as strong as the bonds in the initial reagents, most likely being of a noncovalent nature. However, fragmentation is sometimes observed when multiple collisions are allowed, or when the ion that is collisionally dissociated is given more kinetic energy, such as fragmentation of $[VO(MMA)]^{+}$ to give $[VO(CH_2O)]^{+}$ and of $[VO(MMA)_2]^{+}$ to give $[VO(MMA)(MMA-CH_3O)]^{+}$, as well as fragmentation of $[VO(DMMA)]^{+}$ by loss of fragments of the DMMA adduct.

5. Conclusion

For the three sets of reactions studied, VO^{+} with MIB, MMA, and DMMA, respectively, the complexity of the product distribution increases with the number of electron rich sites on the reagent molecule.

Two sets of primary ion products are observed: (a) protonated reagent molecules and their corresponding stable fragments formed by loss of CH_4O; and (b) products containing VO, formed by addition of whole reagent molecules or associated fragments. The final products are a result of both consecutive and parallel reactions. The decay of the parent ion describes a pseudo-first order reaction, which indicates that one process is responsible for its removal, the formation of an intermediate addition product. CID experiments reveal that the [VO − whole reagent molecule] bonds are of a noncovalent nature, whereas for the smaller [VO + reagent molecule fragment] ions, rearrangement is believed to occur, resulting in much more strongly bound complexes. It is proposed that binding of the reagent molecule fragment(s) to VO is via the methoxy oxygen, whereas interaction with whole reagent molecules could also be the result of interactions with the π-electron system of the conjugated double bond(s).

One motivation for this study was to assess whether the vanadium monoxide cation performs a catalytic function in the polymerization of methyl methacrylates. We cannot dismiss the production of polymeric species in these reactions, however, if they were produced they were not in an ionized form, and thus not able to be detected in our instrument.

6. Note

The VO^+ ion has a $^3\Sigma^-$ ground state ~7.2 eV above the ground state of VO ($^4\Sigma^-$), with some of the lower excited states of VO^+ being a $^3\Delta$ (1.17 eV above the $^3\Sigma^-$), a $^3\Phi$ (~0.08 eV above the $^3\Delta$), two $^3\Pi$ (within ~0.7 eV of $^3\Delta$), a singlet $^1\Delta$, and two quintuplet states ($^5\Pi$ and $^5\Sigma^-$ ~10.5 eV and ~11 eV above the ground state of VO, respectively) [39–44]. The ionization energies of methyl isobutyrate and methyl methacrylate have been estimated at 9.9–10.3 eV and 9.7–10.3 eV [45], respectively, whereas no information on DMMA was available. No reference with respect to the ionization energy to the singlet ($^1\Delta$) state of VO^+ was obtained.

Acknowledgements

G.D.W. wishes to express his sincere thanks to Professor Jim Morrison for his guidance and support over the last 29 years. As Foundation Professor of Chemistry at La Trobe University, Jim has always been very supportive of his students and colleagues, and his work has provided great inspiration to those of us working in the field of mass spectrometry.

This work has been supported by grants from the Australian Research Council, and by an Australian Postgraduate Award, and a Research Scholarship from the School of Chemistry, UNSW to A.D.

References

[1] R.C. Bell, K.A. Zemski, K.P. Kerns, H.T. Deng, A.W. Castleman, J. Phys. Chem. 102 (1998) 1733.
[2] R. Bell, K. Zemski, A. Castleman, J. Phys. Chem. 102 (1998) 8293.
[3] K.J. Fisher, D.R. Smith, G.D. Willett, Proceedings of the 39th ASMS Conference on Mass Spectrometry and Allied Topics, Nashville, TN, 1991, p. 37.
[4] A. Dinca, T. Davis, K. Fisher, D. Smith, G. Willett, Int. J. Mass Spectrom. 183 (1999) 73.
[5] B. Grzybowska-Swierkosz, F. Trifiro, J.C. Vedrine (Eds.), Vanadia Catalysts for Selective Oxidation of Hydrocarbons and Their Derivatives, Applied Catalysis-A General 157 (1997) issue 1-2.
[6] H.H. Kung, Transition Metal Oxides: Surface Chemistry and Catalysis; Studies in Surface Science and Catalysis, Elsevier, 1989, Vol. 45.
[7] M. Chisholm, Chem. Br. 34 (1998) 33.
[8] T.P. Davis, O. Olabisi, M. Dekker (Eds.), The Handbook of Thermoplastics, Ch. 9.
[9] T.P. Davis, D.M. Haddleton, S.N. Richards, J. Macromol. Sci. Rev. Chem. C 34 (1994) 243.
[10] T.P. Davis, D. Kukulj, D.M. Haddleton, D. Maloney, Trends Polym. Sci. 3 (1995) 365.
[11] H. Yasuda, H. Yamamoto, M. Yamashita, K. Yokota, A. Nakamura, S. Miyake, Y. Kai, N. Kanehisa, Macromolecules 26 (1996) 7134.
[12] H. Yasuda, E. Ihara, Bull. Chem. Soc. Jpn. 70 (1997) 1745.
[13] K. Eller, H. Schwarz, Chem. Rev. 91 (1991) 1121.
[14] D. Schroder, H. Schwarz, Angew. Chem. Int. Ed. Engl. 34 (1995) 1973.
[15] R.C. Dunbar, G.T. Uechi, B. Asamoto, J. Am. Chem. Soc. 116 (1994) 2466.
[16] K. Seemeyer, D. Schroder, M. Kempf, O. Lettau, J. Muller, H. Schwarz, Organometallics 14 (1995) 4465.
[17] D. Schroder, H. Schwarz, D.E. Clemmer, Y.M. Chen, P.B.

Armentrout, V.I. Baranov, D.K. Bohme, Int. J. Mass Spectrom. Ion Processes 161 (1997) 175.
[18] S.Z. Kan, Y.C. Xu, Q. Chen, B.S. Freiser, J. Mass Spectrom. 32 (1997) 1310.
[19] Y.M. Chen, M.R. Sievers, P.B. Armentrout, Int. J. Mass Spectrom. Ion Processes 167 (1997) 195.
[20] A. Bjarnason, D.P. Ridge, Organometallics 17 (1998) 1889.
[21] C. Berg, M. Beyer, U. Achatz, S. Joos, G. Niednerschatteburg, V.E. Bondybey, J. Chem. Phys. 108 (1998) 5398.
[22] J.K. Gibson, J. Vac. Sci. Technol. A 16 (1998) 653.
[23] E.F. Fialko, A.V. Kikhtenko, V.B. Goncharov, K.I. Zamaraev, J. Phys. Chem. 101 (1998) 8607.
[24] G.S. Jackson, F.M. White, C.L. Hammill, R.J. Clark, A.G. Marshall, J. Am. Chem. Soc. 119 (1997) 7567.
[25] O. Gehret, M.P. Irion, Chem. Phys. Lett. 254 (1996) 379.
[26] S.Z. Kan, S.A. Lee, B.S. Freiser, J. Mass Spectrom. 31 (1996) 62.
[27] C.Q. Jiao, B.S. Freiser, J. Phys. Chem. 99 (1995) 10 723.
[28] C.Q. Jiao, B.S. Freiser, J. Phys. Chem. 99 (1995) 3969.
[29] P.F. Greenwood, M.G. Strachan, G.D. Willett, M.A. Wilson, Org. Mass Spectrom. 25 (1990) 353.
[30] T.H. Nguyen, P.S. Clezy, G.L. Paul, J. Tan, G.D. Willett, P.J. Derrick, Org. Mass Spectrom. 26 (1991) 215.
[31] R.B. Cody, R.C. Burnier, B.S. Freiser, Anal. Chem. 54 (1982) 96.
[32] C.E.C.A. Hop, T.B. McMahon, G.D. Willett, Int. J. Mass Spectrom. Ion Processes 101 (1990) 191.
[33] M.J. Frisch, G.W. Trucks, H.B. Schlegel, G.E. Scuseria, M.A. Robb, J.R. Cheeseman, V.G. Zakrzewski, J.A. Montgomery, R.E. Stratmann, J.C. Burant, S. Dapprich, J.M. Millam, A.D. Daniels, K.N. Kudin, M.C. Strain, O. Farkas, J. Tomasi, V. Barone, M. Cossi, R. Cammi, B. Mennucci, C. Pomelli, C. Adamo, S. Clifford, J. Ochterski, G.A. Petersson, P.Y. Ayala, Q. Cui, K. Morokuma, D.K. Malick, A.D. Rabuck, K. Raghavachari, J.B. Foresman, J. Cioslowski, J.V. Ortiz, B.B. Stefanov, G. Liu, A. Liashenko, P. Piskorz, I. Komaromi, R. Gomperts, R.L. Martin, D.J. Fox, T. Keith, M.A. Al-Laham, C.Y. Peng, A. Nanayakkara, C. Gonzalez, M. Challacombe, P.M.W. Gill, B.G. Johnson, W. Chen, M.W. Wong, J.L. Andres, M. Head-Gordon, E.S. Replogle, J.A. Pople, GAUSSIAN 98 (Version 5.1), Gaussian, Inc., Pittsburgh, PA, 1998.
[34] C. Lee, W. Yang, R.G. Parr, Phys. Rev. A 37 (1998) 785.
[35] A.D. Becke, Phys. Rev. A 38 (1988) 3098.
[36] B. Miehlich, A. Savin, H. Stoll, H. Preuss, Chem. Phys. Lett. 157 (1989) 200.
[37] A.D. Becke, J. Chem. Phys. 98 (1993) 5648.
[38] D.E. Clemmer, N. Aristov, P.B. Armentrout, J. Phys. Chem. (1993) 544.
[39] J.M. Dyke, B.W.J. Gravenor, M.P. Hasting, A. Morris, J. Phys. Chem. 89 (1985) 4613.
[40] E.A. Carter, W.A. Goddard, J. Phys. Chem. 92 (1988) 2109.
[41] A.J. Merer, Annu. Rev. Phys. Chem. 40 (1989) 407.
[42] M.R. Sievers, P.B. Armentrout, J. Chem. Phys. 102 (1995) 754.
[43] E. Broclawik, Catal. Today 3 (1995) 379.
[44] E. Broclawik, Int. J. Quantum Chem. 56 (1995) 779.
[45] S.G. Lias, J.F. Liebman, R.D. Levin, S.A. Kafafi (Eds.), S.E. Stein (Software), NIST Positive Ion Energetics (Version 2.0), National Institute of Standards and Technology, Gaithersburg, MD, 1993.